The Stellar Population, 3D structure, and kinematics of the Galactic bulge

M. Zoccali[1,2]

[1] *Instituto de Astrofísica, Pontificia Universidad Católica de Chile, Santiago, Chile*
[2] *Millennium Institute of Astrophysics, Santiago, Chile*

Contact / mzoccali@astro.puc.cl

Resumen / Nuestro entendimiento de la estructura y la población estelar del bulbo Galáctico ha mejorado significativamente en los últimos ∼5 años, gracias a mapeos fotométricos en el infrarrojo como el VISTA Variables in the Vía Láctea (VVV Minniti et al., 2010) junto a campañas masivas de observación espectroscópicas como ARGOS, Gaia ESO, GIBS y APOGEE. Presento aquí una versión muy resumida y simplificada, proveniente de una charla invitada dirigida a colegas chilenos y argentinos que trabajan en distintas áreas de la astrofísica. Este trabajo, lejos de representar una revisión completa de la literatura, se propone guiar al lector hacia las interpretaciones que actualmente logran el máximo consenso en la comunidad. La reciente conferencia sobre "The Galactic bulge at the crossroads" organizada en Pucón, Chile, en diciembre 2018 me ha ayudado mucho en obtener esa visión global. Este artículo, entonces, es recomendado para alumnos jóvenes o colegas de otras áreas. Para una visión más completa se recomienda el artículo de Barbuy et al. (2018), o la edición 2016 de *Publication of the Astronomical Society of Australia*, que incluye una sección especial dedicada a artículos de revisión sobre el bulbo Galáctico.

Abstract / Our understanding of the structure and stellar population of the Galactic bulge has improved significantly in the last ∼5 years or so, thanks to large near infrared photometric surveys such as the VISTA Variables in the Vía Láctea (VVV Minniti et al., 2010) coupled to massive spectroscopic campaigns such as ARGOS, Gaia ESO, GIBS and APOGEE. I provide here a summarized and simplified overview, proceeding from an invited review talk delivered to Chilean and Argentinian colleagues from many different fields of astrophysics. The present short paper, far from providing an extensive review of the literature, is meant to point the reader towards the interpretations that currently obtain the widest consensus in the community. The recent conference on "The Galactic bulge at the crossroad", held in Pucón, Chile, in December 2018 greatly helped me draw this global picture. This paper is therefore recommended for young students and/or outsiders to this topic. For a complete review, I refer the readers to Barbuy et al. (2018), and to the 2016 issue of the Publication of the Astronomical Society of Australia, including a special section dedicated to review papers on Galactic bulge.

Keywords / stars: abundances — Galaxy: bulge — Galaxy: stellar content

1. Introduction

The Milky Way galaxy includes three main stellar components, in order of decreasing mass: the disk, the bulge and the halo. It should be noted that the word "bulge" here indicates whatever its included within a radius of ∼2.5 kpc (by some authors up to 3.5 kpc) from the Galactic center, independent from its shape. Bulge and halo are the oldest ones, according to our understanding, with the halo being possible older than the bulge. The disk, with its $\sim 6\times10^{10}$ $M_\odot$ is between 3 and 4 times more massive than the bulge, and about 100 times more massive than the halo. It is, however, a relatively younger component that has formed stars from ∼ 10 Gyr ago down to the present time. For this reason, in order to understand how did the Milky Way form, as a whole, the bulge plays a crucial role, being at the same time massive and old. In other words, it is the first massive stellar component to be set in place.

It is also the only galaxy bulge that can be resolved into individual stars down to the faintest ones, and for which detailed chemical abundances can be obtained through high resolution spectra at least for its giants. It might be used, therefore, as a bridge to try and solve the tension currently present between the formation scenarios proposed to explain local bulges, and the interpretation of the observations of star forming bulges at high redshift.

Specifically, following the review paper by Kormendy & Kennicutt (2004), local bulges have been morphologically classified into *classical* and *pseudo*-bulges. The first ones, more spheroidal and massive with respect to the disk, are interpreted as formed via violent dissipationless merging of primordial subunits. *Pseudo*-bulges instead, including bars and smaller structures with kinematical signatures similar to small disks, are interpreted as the natural product of the dynamical evolution of disks, as the instabilities induced by spiral arms drive stars towards the center, arranging most of them in elongated orbits supporting bars. Theoretical simulations (Debattista et al., 2017; Tissera et al., 2018; Fragkoudi et al., 2018) prove that both scenarios can occur, and would form central bulges with several properties com-

patible with the observed ones. Both scenarios, however, assume that most of the stars currently in the bulge have been formed elsewhere, either in external subunits or in the disk, and have been driven to their current position on a second time, by some independent mechanism.

The two scenarios mentioned above are probably two extremes, with reality being some combination of both phenomena. Both of them, however, as well as any combination of them, contrast with observations of star forming galaxies at redshift ∼2, corresponding to ∼10 Gyr ago, when the bulk of bulge stars must have formed. Studies of these infant galaxies at several wavelengths (e.g., Tadaki et al., 2017) show that they are undergoing a starburst phase at their center, i.e., stars are forming, very efficiently, already at their final position in the bulge. Similar conclusions are reached by e.g. Immeli et al. (2004); Carollo et al. (2007); Elmegreen et al. (2008); Genzel et al. (2008); Bournaud et al. (2009)

2. The three dimensional structure of the Galactic bulge

Fig. 1 shows an artistic image of the Milky Way, as seen from the Northern Galactic Hemisphere, released from NASA in 2017 and reflecting the latest result from the infrared Spitzer satellite. It can be seen that the central region contains a bar. This was first suggested by de Vaucouleurs (1964), as a possible cause for the non-circular motions of the gas in the inner Galaxy, and later confirmed by Blitz & Spergel (1991), as a way to explain the asymmetries in the near infrared light profile of the bulge. Since then, at least a few dozen independent studies have confirmed the existence of a bar at the center of the Milky Way and have determined its main parameters, most often by using core Helium burning stars in the red clump (RC), as distance indicators. Among them, I believe that the most accurate are the ones derived by Wegg & Gerhard (2013) and Simion et al. (2017) from VVV data. They perform a thorough modeling of the most homogeneous, deep and complete photometric data currently available for the bulge. Wegg & Gerhard (2013), in particular, derive an axis ratio of (10:6.3:2.6), exponential scalelengths (0.70:0.44:0.18) kpc and inclination angle with respect to the Sun-Galactic center direction of 27°. They also model the appearance of a boxy/peanut (B/P) structure in the outer bulge, starting from ∼400 pc from the Galactic plane, whose existence was first discovered by McWilliam & Zoccali (2010) and Nataf et al. (2010). The latter B/P structure, sometime referred as the *X-shape*, has also been seen directly in the bulge maps obtained from the WISE satellite as processed by Ness & Lang (2016).

Much before discovering the existence of a B/P structure in our own Galaxy, such features had been seen in nearby galaxies, and their nature and origin was well understood. Once bars are formed, they often undergo dynamical instabilities that produce bending, up or down the plane, of the most elongated orbits, turning them into *bananas*, or *smiles* and *frawns*. This process,

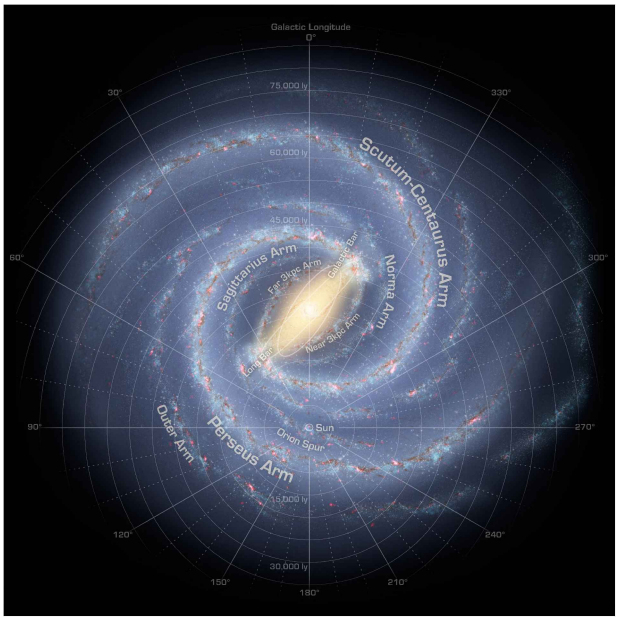

Figure 1: The most accurate artistic image of the Milky Way, reflecting the results from the GLIMPSE survey, on the Spitzer Telescope. The central region includes a prominent bar, with two major arms (Scutum-Centaurus and Perseus) attached to its ends. Another two minor arms are located between the major ones. Image credit: NASA/JPL-Caltech/R. Hurt (SSC/Caltech).

also called buckling, thickens the bar bringing stars away from the plane, while the *smiles* and *frawns* orbits sustain the B/P, or X-shape (Patsis et al., 2002; Athanassoula, 2005). The observational evidence pointing to the existence of a B/P structure in the Milky Way is the fact that the bulge RC magnitude changes smoothly across the bulge area, as the line of sight crosses the near or the far side of the bar, and the RC becomes double in a few specific directions, where the line of sight crosses two arms of the X-shape. Alternative explanations for the change in the magnitude of the RC have been proposed by Lee et al. (2015); Joo et al. (2017), invoking the presence of two populations of stars in the bulge, with different helium abundance, hence different RC magnitude. One of the two, and only occasionally both, prevails in different lines of sights with a complicate fine-tuning of their spatial distribution.

Dynamical models following the secular evolution of galactic bars predicts that only the central part of the bar thickens due to bending and buckling instabilities, leaving a thin, longer bar in the outer part. This structure has been identified in the Milky Way by different authors, starting from Hammersley et al. (1994, 2000), later followed by, e.g., Benjamin et al. (2005); López-Corredoira et al. (2007); Cabrera-Lavers et al. (2007, 2008). It was long debated whether the long bar was a different structure, formed independently from the main bar, or part of the same one. The fact that the inclination angle of the long bar seemed to be different from the one of the main bar added confusion and disagreement to the matter. The debate seems finally settled after Wegg et al. (2015), who were able to fit a combination of

data from UKIDSS, VVV, 2MASS and GLIMPSE with a single model, shown in Fig. 2, including the main bar, the B/P and the long bar. The similarity between the best fit model in Fig. 2 and the output of the dynamical models of bar evolution shown by Athanassoula et al. (2015, their Fig. 4) is a strong argument in favor of a single process giving rise to the bar, the B/P and the thin long bar in our Galaxy.

The central $\pm 1^\circ$ from the Galactic center have always been challenging both to the observations, due to high stellar density and foreground obscuration, and to any attempt at fitting the same bar model reproducing the bar far from the center. Alard (2001) first proposed that the large residuals obtained in the attempt to deproject 2MASS star counts could be explained by the existence of an inner bar, a separate component with a different inclination angle. Many other studies have confirmed the existence of a change in the bar inclination angle in the innermost $\sim 1^\circ$, including Rodriguez-Fernandez & Combes (2008); Nishiyama et al. (2005); Gonzalez et al. (2011). Gerhard & Martinez-Valpuesta (2012) demonstrated that the observed change in angle could also be explained by a central axisymmetric structure, rather than an inner bar. Recent observational evidences support this latter hypothesis, as the inner region of the Galaxy, roughly included within a radius of ~150 pc, shows a high stellar density peak that seems roundish both in the plane of the sky (Valenti et al., 2016) and in the Galactic plane (Zoccali & Valenti, 2016). We will come back on the peculiarities of the innermost region of the bulge when discussing the stellar kinematics, in Sect. 5. below. For a more complete review about the bulge 3D structure, the reader should refer to Zoccali & Valenti (2016).

3. The bulge stellar mass and density distribution

The distribution of RC stars in the plane of the sky, as measured from VVV catalogs corrected for completeness and interstellar extinction was used by Valenti et al. (2016) to derive the stellar density profile of the bulge. Their map shows the known asymmetries, signature of the bar, but also the central high density peak mentioned above. The same authors derived an empirical conversion factor between the number of RC stars and the total stellar mass. The latter was measured by integrating the empirical initial mass function (IMF) by Zoccali et al. (2000); Zoccali et al. (2003) within a small field observed with *HST*. This factor allowed to transform the projected density of RC stars per square degrees into total stellar mass, hence derive both a mass profile and a total stellar mass for the Galactic bulge, resulting into 2×10^{10} $M_\odot$.

An alternative, more conventional way to measure the total mass of a system is the matching of the stellar three dimensional (3D) density profile and kinematics within a self consistent dynamical model. This has been done recently by Portail et al. (2015, 2017) who concluded that the total mass within a volume of ($\pm 2.2 \times \pm 1.4 \times \pm 1.2$ kpc) is $1.84 \pm 0.07 \times 10^{10}$ $M_\odot$. This

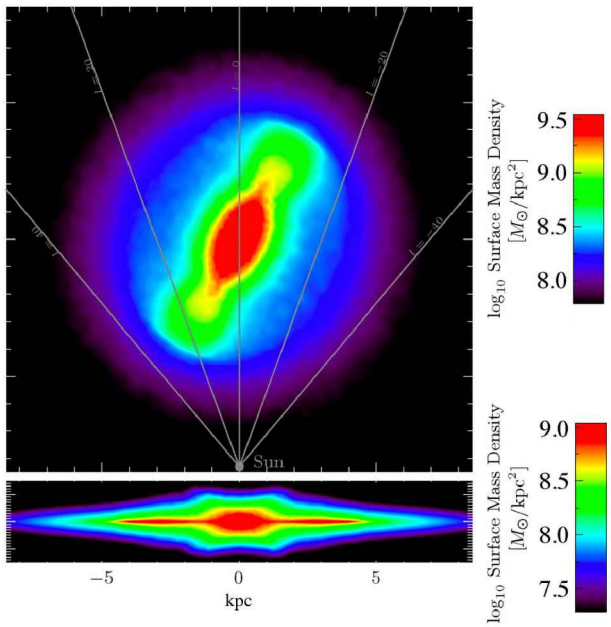

Figure 2: Best fitting model reproducing the Galactic bar (central oval in red) with its B/P structure sticking out at large distances from the plane, clearly visible in green in the lower panel. Also shown is the long bar, as a thin structure (in red) extending to large longitudes. Adapted from Wegg et al. (2015).

obviously includes the dark matter component, while the stellar part is estimated to be between 1.25 and 1.6×10^{10} $M_\odot$.

The apparent inconsistency between these two results is most likely due to the fact that Valenti et al. (2016) estimates the mass of all the stellar population along the line of sight contributing to the observed RC, in the region of the sky comprised within $-10^\circ < l < 10^\circ$ and $-10^\circ < b < 10^\circ$. Portail et al. (2015), on the contrary, define a box with axis proportional to the main bar axis, that corresponds to a smaller volume of space.

In any case, the current accuracy in the determination of the bulge stellar mass allows us to establish beyond any doubt that the Galactic bulge is a massive stellar component of the Milky Way, making up about 1/4 of the total stellar mass. In addition, regardless of the absolute calibration of the total mass, the projected stellar density and mass *profiles*, which only depend on the variation of the number of RC stars across the sky, are both robust determinations, given that the VVV photometry is mostly complete at the magnitude of the RC. These will be used further below in order to characterize the shape of the two metallicity components of the Galactic bulge.

4. Two metallicity components in the Galactic bulge

The metallicity distribution function (MDF) of bulge stars was first measured by McWilliam & Rich (1994), in the low reddening Baade's Window, at (l, b)=(1, −4).

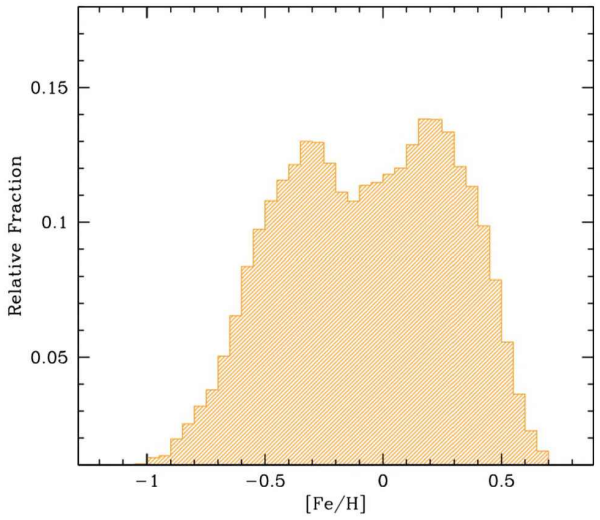

Figure 3: Metallicity distribution function of all the stars measured within the GIBS survey (Zoccali et al., 2017). The existence of a bi-modality is very evident, with the metal poor component centered at [Fe/H]=−0.4 dex and the metal rich one centered at [Fe/H]=+0.3 dex.

They concluded that most bulge stars had roughly solar metallicity, with a sharp decline at super solar metallicity and a longer tail towards the metal poor regime. For almost two decades this MDF was assumed to be representative of all the stars in the bulge, with a mean metallicity gradient hard to quantify but qualitatively close to a decrease by about 0.6 dex per kpc, towards higher latitudes (e.g. Zoccali et al., 2008).

Recent wide area spectroscopic surveys allowed us to map the MDF in several line of sights across the bulge area (Ness et al., 2013a; Rojas-Arriagada et al., 2014, 2017; Zoccali et al., 2017). The results proved that the sub-solar metallicity tail seen by McWilliam & Rich (1994) was in fact a second component. Indeed, when measured with increased statistics and precision, the bulge MDF is everywhere bimodal, with a metal-poor peak at [Fe/H]~ -0.4 dex and a metal rich one at [Fe/H]$\sim$+0.3 dex (Fig. 3). The position of the two peaks does not change across the bulge area, but their relative importance does change significantly, with metal rich stars largely dominating at intermediate latitudes ($\sim$70 % of the total at $b = -3.5°$ and metal poor ones dominating in the outer part ($\sim$70 % at $b = -8.5°$). At latitude closer to the Galactic plane, the relative importance of the metal poor component increases again (Schultheis et al., 2015; Zoccali et al., 2017; Feldmeier-Krause et al., 2017) though its relative contribution is somewhat poorly quantified, due to the difficulties to measure a large number of stars at high spectral resolution in the innermost, high extinction regions of the Galaxy.

The two metallicity components seem to have different properties also in space distribution and kinematics. By analyzing the luminosity function of the target RC stars belonging to each component Ness et al. (2012); Rojas-Arriagada et al. (2014) demonstrated that the metal poor stars do not show the split RC identified in the metal rich ones at $|l| < 2°$, $|b| < 5°$, and interpreted as the observational signature of the B/P structure. On a further analysis by Rojas-Arriagada et al. (2017), the magnitude of the metal poor RC stars turned out to be constant with longitude, at fixed latitudes, contrary to the behavior of metal rich stars, brighter at positive longitudes, where the line of sight crosses the near side of the Galactic bar. These results, then, point towards the bar being made only by metal rich stars, while metal poor ones are found at the same mean distance across all longitudes, therefore tracing a more axisymmetric structure.

Independent confirmation of the same result came from Zoccali et al. (2017). While their RC target box was too small to analyse the luminosity function, they coupled the metal-poor/metal-rich fraction given by the MDF in each of 26 fields with the projected total stellar density in Valenti et al. (2016). This allowed them to derive two separate density maps, tracing each of the two metallicity components individually. The projected distribution of metal rich stars is a well defined rectangular box, as expected for a bar seen edge-on, while the distribution of metal poor stars is roundish, consistent with the projection in the sky of an axisymmetric structure such as a spheroid. Integration of both density maps over the whole bulge area yields a relative contribution to the bulge total mass close to 50 % for each of the two components (Zoccali et al., 2018).

While it is reasonably established that the bulge hosts two components with different shape, metallicity distribution, element ratio, and —as discussed below— kinematics, it is not clear whether they formed via a completely different process, or via the same one, at work under different conditions. While there is only one mechanism currently known to produce galaxy bars, the final shape (axis ratio) of the bars strongly depends on the radial velocity dispersion of the initial disk (Debattista et al., 2017; Fragkoudi et al., 2018). Specifically, a disk with large velocity dispersion along the radial direction such as a hypothetical primordial disk in the Milky Way, would give rise to a much less pronounced bar, compatible with the *spheroidal* distribution observed for metal poor stars. Obviously, such axisymmetric structure could also be a *classical bulge* resulting from the violent accretion of galactic fragments at early times. Models have not yet been able to identify observational features able to discriminate between the two scenarios.

For a more complete review about the bulge metallicity distribution the reader should refer to Ness & Freeman (2016), while a highly recommended review more specific on the bulge chemical composition and evolution can be found in McWilliam (2016).

4.1. ...or three?

One of the main products of both the OGLE III (Soszyński et al., 2011) and the VVV survey has been the identification and characterization of a large number of RR Lyrae (RRL) variable stars in the Galactic bulge. These variables are clean tracers of the oldest stellar population (> 10 Gyr) and, because they obey a

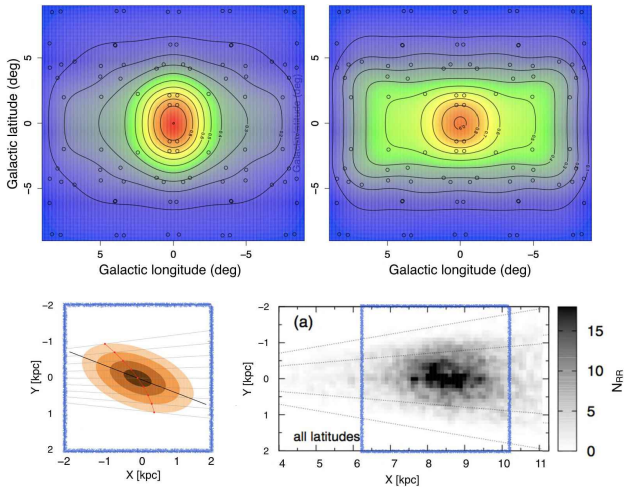

Figure 4: Top: projected stellar density maps, in the plane of the sky, for the metal poor (left) and the metal rich (right) components of the Galactic bulge, from GIBS (Zoccali et al., 2017). Bottom: density of RR Lyrae projected on the Galactic plane. The optical data from the OGLE survey (left, from Pietrukowicz et al., 2015) show an elongated structure very similar to the Galactic bar, while the combination of OGLE with VVV near infrared data (right, from Dékány et al., 2013) show a roundish structure, with no trace of elongation in the direction of the bar major axis.

tight Period-Luminosity relation, each of them yields a precise measure of its distance. It is therefore straightforward, at least in principle, to deproject their stellar density in the sky into a 3D density distribution.

In practice, two groups have attempted to do so using the OGLE III optical data (Pietrukowicz et al., 2015) or their combination with VVV near infrared data (Dékány et al., 2013), respectively, with contrasting results. While the former authors find that RRL variables trace a bar only slightly less elongated than the main bar traced by RC stars, the latter find a rather spheroidal component (Fig. 4). A similar result was obtained by Gran et al. (2016) using only near infrared VVV data for newly identified RRL stars in the outer bulge. The discrepancy is most likely due to the choice of the extinction law, as interstellar reddening is invariably tight to the determination of distances, and it obviously affects different photometric bands in a different way. Although the distance to each individual RRL is of course much more precise than the distance to each individual RC star, the number of RRL in the bulge is several orders of magnitudes lower than the number of RC stars, and therefore small systematics that might vary with longitudes end up having a large effect on the final results. In particular, the amount of foreground dust in the bulge direction is slightly larger at negative longitudes than it is at positive ones, at least close to latitude $b = -3°$ that is where the density of RRL is largest. Outside this region the RRL are intrinsically less abundant, as the whole stellar density declines, while inside this region the OGLE III survey has mapped only the region close to the bulge projected minor axis ($l \sim 0$).

Other independent indications, however, suggest that RRL trace a different component from RC stars, and they come from the kinematics. Indeed, Kunder et al. (2016) measured the radial velocity of ∼1000 RRL in the bulge, deriving a flat rotation curve and a radial velocity dispersion larger than that of RC stars (see Sec. 5.). This would be an argument in favor of a spheroidal distribution of RRL, as spheroids are supported by velocity dispersions, while bars are supported by rotation.

Although the space distribution and 3D kinematics of RRL remains to confirmed, if one temporarily accepts the result that RRL trace a spheroidal component with little or no rotation, a natural question would be: *do RRL trace the same spheroidal component as metal poor RC stars, or are they part of a third one?*. While I believe that this question is still open, a few considerations might be of help. First, the metallicity distribution of RRL, though very broad, peaks at [Fe/H]=−1.0 dex, while metal poor RC stars have their metallicity peak at [Fe/H]=−0.4 dex. However it is also expected that RRL, in order to pulsate, need to fall on the instability strip, while burning He in their core. That is, they spend their horizontal branch phase at a bluer color than RC stars. Given that metallicity is the *first parameter* determining the color of an old star, while on the horizontal branch, it is perfectly possible that RRL represent the most metal poor tail of the metal poor bulge component. Second, a strong argument in favor of RRL tracing the same component as metal poor RC stars would be represented by the evidence of metal poor RC stars also showing no sign of rotation and a higher velocity dispersion. This will be discussed in the next section.

5. Kinematics

Recent spectroscopic surveys mapping the radial velocity of stars in the Galactic bulge at different longitudes, such as the Bulge Radial Velocity Assay (BRAVA Rich et al., 2007; Howard et al., 2009; Kunder et al., 2012), the Abundances and Radial Velocity Galactic Origins Survey (ARGOS Freeman et al., 2013; Ness et al., 2013b,a), the Giraffe Inner Bulge Survey (GIBS Zoccali et al., 2014, 2017), the Gaia-ESO Survey (GES Gilmore et al., 2012; Rojas-Arriagada et al., 2014, 2017), and the Apache Point Observatory Galactic Evolution Experiment (APOGEE Majewski et al., 2017; Ness & Freeman, 2016) all agree that the bulge shows a high degree of "cylindrical rotation". This means that the radial velocity curve (radial velocity as a function of longitude) is largely independent on latitude, with the rotation speed only slightly increasing closer to the plane (Fig. 5). In particular, Shen et al. (2010) showed that the a pure-disk model galaxy correctly reproduces the observed velocities, as the small increase of the rotation speed towards the Galactic plane is consistent with projection effects.

At the same time, the radial velocity dispersion goes from $\sigma \approx 80$ km/s at latitudes b=−8° to $\sigma \approx 140$ km s^{-1} at b=−1°. The latter value represent, in fact, a high-sigma peak only visible within the inner ∼2° of the Galaxy (i.e., within a radius of ∼240 pc). This peak,

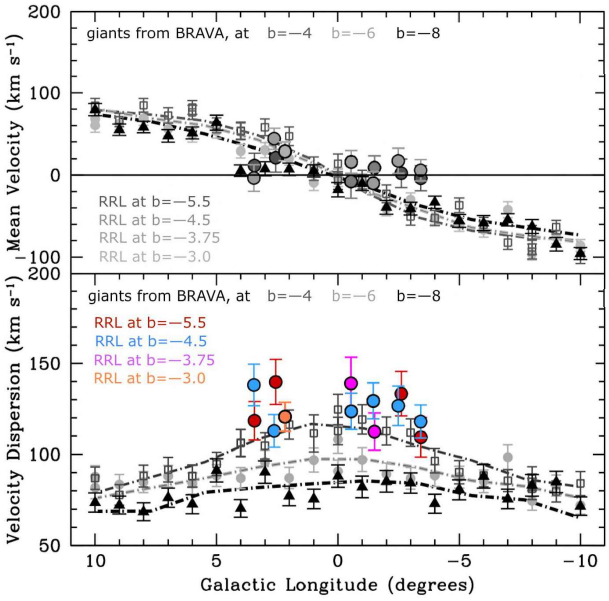

Figure 5: Comparison between the radial velocity profile (top) and the velocity dispersion profile (bottom) for bulge giants measured within the BRAVA survey, shown with black/grey symbols, and for RR Lyrae observed by Kunder et al. (2016), shown with colored symbols. It is clear that RR Lyrae have a flat rotation (top), and a higher velocity dispersion (bottom) compared to other giants. Adapted from Kunder et al. (2016).

mapped by Valenti et al. (2018), spatially coincides with the region where a change in the bar pivot angle had been detected by Alard (2001); Nishiyama et al. (2005); Gonzalez et al. (2011), who interpreted it as evidence for the presence of an inner bar. Later on, Zoccali & Valenti (2016) showed that the data are more consistent with the presence of a central, axisymmetric concentration of stars. It is worth noticing that no model has been shown to reproduce the central peak in velocity dispersion, yet.

As discussed in Sect. 4., spectroscopic surveys with enough resolution to derive stellar metallicities allowed us to identify two stellar components in the bulge, with different mean [Fe/H]. It was quickly evident that the metal rich and metal poor components had, at least, different velocity dispersion trend across the bulge area. Specifically, metal poor stars have higher sigma ($\sim$80 km s^{-1}) than the metal rich ones ($\sim$60 km s^{-1}) in the outer bulge, whereas in the inner few degrees they have lower sigma ($\sim$120 km s^{-1}) compared to the metal rich ones ($\sim$140 km s^{-1}). The global sigma is, of course, close to the metal poor one in the outer bulge, where the metal poor component dominates, and closer to the metal rich one in the inner bulge, where the metal rich dominates. As a word of caution, it should be kept in mind that the two metallicity components have some overlap at intermediate metallicities, therefore some cross-contamination certainly affects the determination of the kinematics of each component individually.

Concerning the rotation velocity pattern, Clarkson et al. (2018) used a combination of broad band filters available on *HST* to distinguish between metal poor and metal rich stars (Renzini et al., 2018), and the magnitude difference between main sequence stars and a mean fiducial line as a proxy for distances. They then used the distribution of proper motions in longitude to demonstrate that metal poor stars rotate significantly slower than metal rich stars. This is consistent with the other evidences that metal poor stars follow a spheroidal distribution, although it would be desirable to confirm this result by means of radial velocities at different longitudes.

Interestingly, Kunder et al. (2016) demonstrated that a sample of $\sim$1000 RR Lyrae variables observed at different longitudes show a high velocity dispersion and a flat rotation curve (see Fig. 5). What still needs to be verified is whether RR Lyrae, tracing the oldest component of the Galactic bulge, belong to the metal poor component described above, or they trace a third, older and more metal poor component. Unfortunately their MDF is not useful to demonstrate whether RR Lyrae and metal poor RC stars belong to the same component, as it is expected that only the most metal poor tail of a population with the MDF of metal poor stars would cross the instability strip, and therefore pulsate, when burning He in their core. The kinematics would be much more informative, but at the moment it is available for a relatively small sample of RR Lyrae and metal poor stars, which makes the results not conclusive yet.

For a more complete review about the bulge kinematics, and its correlation with metallicity, the reader should refer to Babusiaux (2016).

6. The ages of stars in the Galactic bulge

A fundamental information about the origin of the Galactic bulge obviously comes from the age distribution of its stars. While it seems now well established that the age of the bulk of bulge stars is close to 10 Gyr (Ortolani et al., 1995; Zoccali et al., 2003; Valenti et al., 2013; Clarkson et al., 2008; Surot et al., 2019), the actual age distribution, and in particular the size and age of a possible younger population is still strongly debated. The intrinsic difficulty in measuring the age distribution of bulge stars is due to the fact that foreground disk main sequence stars strongly contaminate the bulge turnoff region of the CMD. Decontamination has been attempted both with a statistical approach, using a disk control field, and kinematically, using the fact that the proper motion distribution of foreground disk stars overlaps only partially with that of bulge stars. All the attempts at deriving the age distribution from the shape of the decontaminated turnoff region yielded a population mostly old, with the only exception of Bernard et al. (2018) who find that 10% of bulge stars are younger than 5 Gyr. Independent measurements of the age distribution of bulge stars have been made, in the last 10 years, by Bensby et al. (2017, and references therein). They measured stellar surface parameters (T_{eff} and log g) of individual stars, by means of high resolution spectra obtained while the targets were microlensed (hence significantly brightened) by some unseen foreground object. These parameters, together with the metallicity,

allowed them to place the stars in the theoretical HR diagram, and thus derive their age by comparison with stellar isochrones. The result is that 38% of the sample stars are younger than 8 Gyr, with most of them having super solar metallicity. This percentage represents a factor of 3-4 discrepancy with Clarkson et al. (2008). A recent study by Renzini et al. (2018) uses a combination of *HST* filters to generate metallicity sensitive indices, and therefore separate bulge stars (decontaminated from disk stars by means of proper motions) into metal poor and metal rich ones. The authors found no difference in the magnitude distribution of turnoff stars of both sample. The debate is still open!

7. Summary and Outlook

In the last ∼5 years or so, consensus has been reached that the Galactic bulge is a massive ($1.5-2\times10^{10}M_{\odot}$) component of the Milky Way, including two separate populations. One of them, making up a little more than a half of the total mass, has super solar metallicity, is arranged in a bar that flares up into a peanut, or X-shape, in its outskirt, plus a thin component extended out to ∼4.5 Kpc, confined in the plane. The shape of this component and its kinematics, all indicate a clear disk origin. Another component, with mean metallicity [Fe/H]=−0.4 dex, has a shape very close to a spheroid, higher dispersion and little or no rotation. Its origin is not clear, it might be the result of a violent merging phase, before the bar, or it might also come from an older, hotter disk.

Some of the most significant open problems are the following:

i) Do the RR Lyrae variable trace the same spheroidal component as the metal poor stars? Or do they trace a third, old and metal poor component? Answer to this question will certainly come from the high resolution spectroscopy for tens of thousands of stars enabled by the forthcoming near infrared fibre spectrograph MOONS (Cirasuolo et al., 2014). It will be available at the VLT around 2021, and, among other studies focused on the innermost bulge regions (i.e., the nuclear bulge) it will allow to derive kinematics and metallicities for a large sample of metal poor red clump stars and RR Lyrae.

ii) Is the metal rich component significantly younger than the metal poor one? Addressing this question is harder in my opinion. It requires large statistics, precise (relative) proper motions and metallicities for a large sample of bulge turnoff stars. The first two are already available from *HST* and will certainly improve with the advent of JWHST. The second might have to wait for the 30m class telescopes, and perhaps some more time until multi-object spectrographs will be available on them.

iii) What is the structure and the stellar population of the Nuclear bulge, i.e., the region within $|b|<1°$ and $|l|<3°$. This will most likely be addressed by the high spatial resolution imagers of the JWST and/or the ELTs, together with efficient, near infrared spectrographs such as MOONS.

Acknowledgements: I am grateful to the organizers of the Second Binational Meeting AAA-SOCHIAS for the invitation to deliver the present review talk. I also acknowledge support from the Ministry for the Economy, Development, and Tourism's Programa Iniciativa Científica Milenio through grant IC120009, awarded to Millenium Institute of Astrophysics (MAS), the BASAL CATA Center for Astrophysics and Associated Technologies through grant PFB-06, and from FONDECYT Regular 1150345.

References

Alard C., 2001, A&A, 379, L44
Athanassoula E., 2005, MNRAS, 358, 1477
Athanassoula E., et al., 2015, MNRAS, 454, 3843
Babusiaux C., 2016, PASA, 33, e026
Barbuy B., Chiappini C., Gerhard O., 2018, ARA&A, 56, 223
Benjamin R.A., et al., 2005, ApJL, 630, L149
Bensby T., et al., 2017, A&A, 605, A89
Bernard E.J., et al., 2018, MNRAS, 477, 3507
Blitz L., Spergel D.N., 1991, ApJ, 379, 631
Bournaud F., Elmegreen B.G., Martig M., 2009, ApJL, 707, L1
Cabrera-Lavers A., et al., 2007, A&A, 465, 825
Cabrera-Lavers A., et al., 2008, A&A, 491, 781
Carollo C.M., et al., 2007, ApJ, 658, 960
Cirasuolo M., et al., 2014, *Ground-based and Airborne Instrumentation for Astronomy V*, *Proc. SPIE*, vol. 9147, 91470N
Clarkson W., et al., 2008, ApJ, 684, 1110
Clarkson W.I., et al., 2018, ApJ, 858, 46
de Vaucouleurs G., 1964, F.J. Kerr (Ed.), *The Galaxy and the Magellanic Clouds*, *IAU Symposium*, vol. 20, 195
Debattista V.P., et al., 2017, MNRAS, 469, 1587
Dékány I., et al., 2013, ApJL, 776, L19
Elmegreen B.G., Bournaud F., Elmegreen D.M., 2008, ApJ, 688, 67
Feldmeier-Krause A., et al., 2017, MNRAS, 464, 194
Fragkoudi F., et al., 2018, A&A, 616, A180
Freeman K., et al., 2013, MNRAS, 428, 3660
Genzel R., et al., 2008, ApJ, 687, 59
Gerhard O., Martinez-Valpuesta I., 2012, ApJL, 744, L8
Gilmore G., et al., 2012, The Messenger, 147, 25
Gonzalez O.A., et al., 2011, A&A, 534, L14
Gran F., et al., 2016, A&A, 591, A145
Hammersley P.L., et al., 1994, MNRAS, 269, 753
Hammersley P.L., et al., 2000, MNRAS, 317, L45
Howard C.D., et al., 2009, ApJL, 702, L153
Immeli A., et al., 2004, A&A, 413, 547
Joo S.J., Lee Y.W., Chung C., 2017, ApJ, 840, 98
Kormendy J., Kennicutt Jr. R.C., 2004, ARA&A, 42, 603
Kunder A., et al., 2012, AJ, 143, 57
Kunder A., et al., 2016, ApJL, 821, L25
Lee Y.W., Joo S.J., Chung C., 2015, MNRAS, 453, 3906
López-Corredoira M., et al., 2007, AJ, 133, 154
Majewski S.R., et al., 2017, AJ, 154, 94
McWilliam A., 2016, PASA, 33, e040
McWilliam A., Rich R.M., 1994, ApJS, 91, 749
McWilliam A., Zoccali M., 2010, ApJ, 724, 1491
Minniti D., et al., 2010, NewA, 15, 433
Nataf D.M., et al., 2010, ApJL, 721, L28
Ness M., Freeman K., 2016, PASA, 33, e022
Ness M., Lang D., 2016, AJ, 152, 14
Ness M., et al., 2012, ApJ, 756, 22
Ness M., et al., 2013a, MNRAS, 430, 836
Ness M., et al., 2013b, MNRAS, 432, 2092
Nishiyama S., et al., 2005, ApJL, 621, L105
Ortolani S., et al., 1995, Nature, 377, 701

Patsis P.A., Skokos C., Athanassoula E., 2002, MNRAS, 337, 578
Pietrukowicz P., et al., 2015, ApJ, 811, 113
Portail M., et al., 2015, MNRAS, 448, 713
Portail M., et al., 2017, MNRAS, 470, 1233
Renzini A., et al., 2018, ApJ, 863, 16
Rich R.M., et al., 2007, ApJL, 658, L29
Rodriguez-Fernandez N.J., Combes F., 2008, A&A, 489, 115
Rojas-Arriagada A., et al., 2014, A&A, 569, A103
Rojas-Arriagada A., et al., 2017, A&A, 601, A140
Schultheis M., et al., 2015, A&A, 584, A45
Shen J., et al., 2010, ApJL, 720, L72
Simion I.T., et al., 2017, MNRAS, 471, 4323
Soszyński I., et al., 2011, AcA, 61, 1
Surot F., et al., 2019, arXiv e-prints
Tadaki K.i., et al., 2017, ApJ, 834, 135
Tissera P.B., et al., 2018, MNRAS, 473, 1656
Valenti E., et al., 2013, A&A, 559, A98
Valenti E., et al., 2016, A&A, 587, L6
Valenti E., et al., 2018, A&A, 616, A83
Wegg C., Gerhard O., 2013, MNRAS, 435, 1874
Wegg C., Gerhard O., Portail M., 2015, MNRAS, 450, 4050
Zoccali M., Valenti E., 2016, PASA, 33, e025
Zoccali M., Valenti E., Gonzalez O.A., 2018, A&A, 618, A147
Zoccali M., et al., 2000, ApJ, 530, 418
Zoccali M., et al., 2003, A&A, 399, 931
Zoccali M., et al., 2008, A&A, 486, 177
Zoccali M., et al., 2014, A&A, 562, A66
Zoccali M., et al., 2017, A&A, 599, A12